

Cortical Neuron Outgrowth is Insensitive to Substrate Stiffness

LEANN L. NORMAN and HELIM ARANDA-ESPINOZA

Fischell Department of Bioengineering, University of Maryland at College Park, 3138 Jeong H. Kim Engineering Building, College Park, MD 20742, USA

(Received 23 March 2010; accepted 14 July 2010; published online 30 July 2010)

Associate Editor Christopher Chen oversaw the review of this article.

Abstract—Changes in substrate compliance affect the cellular behavior of numerous cell types including epithelial, endothelial, fibroblasts, and stem cells. Recently, an emphasis has been placed on understanding the mechanotactic behavior of neurons, in an attempt to treat neurological injury and disease as well as to optimize the development of synthetic biomaterials for neural regeneration. Here, we determine the stiffness of the fetal rat cortex using atomic force microscopy and evaluate the effect of substrate mechanics on cortical neuron behavior using polyacrylamide gels with stiffness around that measured for the cortex. In particular, we evaluate the relationship between substrate compliance and ligand coating to morphology, differentiation, and extension behavior. Remarkably, we see an insensitivity of cortical process length and migration to substrate stiffness. We observe differences in the tortuosity of process extension on laminin vs. poly-D-lysine, as well as differences in cell body migration; however these differences are independent of substrate compliance. Myosin II inhibition revealed effects independent of stiffness, yet dependent on outgrowth behavior. Collectively, this work suggests that cortical neurons are capable of differentiating and extending processes regardless of substrate stiffness, which we attribute to the homogeneity of their native environment and their unwarranted need to distinguish substrate compliance.

Keywords—Mechanotaxis, Axon differentiation, Polyacrylamide gels, Atomic force microscopy.

INTRODUCTION

Critical correlations between matrix stiffness and disease, including the stiffening of tissue in cancer tumors,⁴⁶ changes in stiffness during the process of liver fibrosis,²³ and the hardening of arteries in atherosclerosis^{39,40} have generated a vast amount of research aimed at understanding how these physical alterations

affect cellular behavior and disease. Substrate stiffness has shown impacting effects on cell behavior, including migration and morphology for an assortment of cell types including epithelial,⁴⁷ endothelial,⁶⁵ vascular smooth muscle,^{8,63} fibroblasts,^{47,65} neutrophils,⁵⁶ and stem cells.^{16,53,54} Understanding the way in which substrate stiffness affects these cellular responses may shed light onto how to treat and/or prevent diseases which involve changes in matrix compliance.

Recently, attempts aimed at understanding the effect of substrate stiffness on neuronal cells has been of significant interest, in particular, for understanding embryonic development and for designing tissue engineered materials for central nervous system injury and disease.⁴³ To date, published studies have shown contrasting effects of substrate compliance on neurite outgrowth, with some reporting increases in the rate of neurite outgrowth² and branching¹⁸ with decreased gel stiffness, while others report decreases in outgrowth and branching³³ with decreased compliance. In contrast, for cortical neurons grown in an astrocyte/neuron co-culture, there were no differences in axon length due to substrate compliance, however differences in actin assembly were observed.²² Numerous factors which likely influence these discrepancies include physical differences such as variations of substrate stiffness or dimensionality (i.e., 2D vs. 3D), as well as differences in signaling which may arise from variations in ligand selection and concentration, as well as culture conditions. Also, the age and class of neurons, cell density, as well as time and length of observation, are variables that could account for differences in observed behaviors.

When evaluating substrate compliance, most studies select a range of stiffness that covers a general span of the native tissue. However, these “native” compliance ranges, typically gathered from literature, can vary between animal of origin, tissue type and preparation, as well as testing method.³⁵ For example, the elastic modulus of swine brain has been reported between 260

Address correspondence to Helim Aranda-Espinoza, Fischell Department of Bioengineering, University of Maryland at College Park, 3138 Jeong H. Kim Engineering Building, College Park, MD 20742, USA. Electronic mail: helim@umd.edu

and 490 Pa,⁴² while a more detailed evaluation of the rat brain revealed a heterogeneity among the hippocampus with stiffness ranging between 137 and 308 Pa using AFM and 662 Pa using macroscopic testing methods.¹⁵ This is in sharp contrast to other neuron-rich environments, such as the spinal cord, which has been measured at 89 kPa for human,⁴¹ yet dramatic variations in mechanical properties are observed among other vertebrates.¹⁰ In addition to differences among species, variation in the mechanical properties of animals also differs with age. For instance, Clarke *et al.*¹¹ observe an increase in elastic modulus for adult rat compared to neonatal spinal cord, while Prange and Margulies⁴⁹ report an increase in the shear relaxation modulus of infant vs. adult brain. This suggests the likelihood that stiffness changes during development are tissue dependent, and in the case of neuron-rich tissues, can also depend on the amount of gray vs. white matter since mechanical properties of these areas are known to differ as well.²⁶ In addition to determining the stiffness of native tissue, the compliance of the cell itself has also been of recent interest. The elastic storage modulus of the growth cones of PC12s (neuron-like cells) was reported at approximately 300 Pa, which was the same stiffness at which growth cones were able to detectably deform compliant substrates,¹⁹ illustrating the importance of a cell's own compliance on mechanical impact. The viscoelastic properties of hippocampal and retinal neurons has also been evaluated, with reported elastic modulus ranging between 480 and 970 Pa for hippocampal pyramidal neurons, and 650–1590 Pa for retinal neurons.³⁸ Collectively, the range of mechanical properties reported in the literature illustrate the importance of properly selecting the most appropriate stiffness range when attempting to recapitulate the native environment of the desired cell type.

Here, we determine the stiffness of the E17 fetal rat cortex using atomic force microscopy (AFM) and use the derived Young's modulus to determine an appropriate range of stiffness necessary to evaluate the effect of substrate mechanics on cortical neuron behavior. Using the well-characterized polyacrylamide (PA) gel system, we evaluate the relationship between substrate compliance and ligand coating to morphology, differentiation, and outgrowth behavior of primary cortical neurons. Interestingly, we see an insensitivity of cortical process length and migration to substrate stiffness. We observe differences in the tortuosity of process extension on laminin vs. poly-D-lysine, as well as differences in the cell body migration; however these differences are independent of substrate compliance. Inhibition of myosin II also revealed effects independent of stiffness, yet dependent on extension behavior. Collectively, this work suggests that cortical neurons

are capable of differentiating and extending processes regardless of substrate stiffness. We suspect that at this stage of development, cortical neurons are not mechanotactic due to the homogeneity of their native environment and their unwarranted need to distinguish substrate compliance.

MATERIALS AND METHODS

Preparation of Substrates

Coverslip activation and polyacrylamide gel (PA) preparations were performed according to the methods of Wang and Pelham⁶⁰ and as previously described,⁴⁴ with only slight modifications. Briefly, glass coverslips (22 × 22 mm; Fischer Scientific, Pittsburgh, PA) were coated with 0.1 M NaOH (Fischer Scientific), followed by 3-aminopropyltrimethoxy silane (Sigma, St. Louis, MO). Coverslips were then fixed with 0.5% glutaraldehyde (Sigma) and allowed to air dry. Polyacrylamide gels were prepared with varying concentrations of acrylamide (40% Acryl; Bio-Rad, Hercules, CA), and bisacrylamide (2% Bis; Bio-Rad) using 3 or 8% acrylamide, and 0.04–2% bisacrylamide for final concentrations. A total of 25–35 μ L of gel solution was placed on top of the activated coverslip, and covered with a glass slide (Fisher Scientific) in order to ensure a flat gel. After 30 min of polymerization, the coverslip was removed and the attached gel was measured by microscopy to be approximately 80–100 μ m thick. Sulfosuccinimidyl-6-(4'-azido-2'-nitrophenyl-amino) hexanoate (sulfo-SANPAH, Pierce Chemicals, Rockford, IL) was used to crosslink either 100 μ g/mL poly-D-lysine (PDL; Sigma Aldrich) or 5–40 μ g/mL laminin (Sigma Aldrich) onto the gel surface. Solutions were allowed to incubate on the gel surface for 2 h at room temperature (PDL) or 37 °C (laminin), and were then rinsed three times with PBS.

Determination of Young's Moduli using Dynamic Mechanical Analysis

Dynamic mechanical analysis (DMA) was performed using a Q-800 Dynamic Mechanical Analyzer (TA Instruments, New Castle, DE) and Q Series Explorer software to determine bulk mechanical properties of all PA gels except 3% Acrylamide, 0.06% Bisacrylamide and 3% Acrylamide, 0.04% Bisacrylamide. PA gels measuring 3–4 mm in height were cyclically compressed (1 Hz) to a strain of 1%. Within this strain range, the linear elasticity of PA gels allows for the determination of the Young's modulus. The Young's moduli were determined as the slope of the linear stress–strain curves for each gel. Our reported

Young's moduli are similar to those reported by others for similar concentrations of bis and acrylamide.¹⁸

Determination of Young's Moduli Using Atomic Force Microscopy

Due to the inability to properly size and transfer the extremely soft gels into the Dynamic Mechanical Analyzer, the stiffness of the 3% Acrylamide, 0.06% Bisacrylamide and 3% Acrylamide, 0.04% Bisacrylamide gels was determined using atomic force microscopy (AFM; Agilent, Santa Clara, CA). AFM was performed using a silicon nitride cantilever (Novascan, Ames, IA) with a spherical glass SiO₂ probe of diameter 2.5 μm. Using a glass surface, the deflection sensitivity was measured, while the program Thermal K (Molecular Imaging Corporation, San Diego, CA) was used to measure the spring constant. PA gels attached to glass coverslips were positioned under the AFM tip and force curves were captured for 4–8 regions. This was repeated for 3–5 individual gels. Force curve data was fit with a custom-written Matlab (The MathWorks) program, using the Hertz-Sneddon model for a paraboloid indenter⁶¹:

$$F_{\text{paraboloid}} = \frac{4}{3} \left(\frac{E}{1-\nu^2} \right) R^{1/2} \delta^{3/2}$$

Here, $F_{\text{paraboloid}}$ is the load exerted by the paraboloid indenter and ν is the Poisson's ratio. In this work $\nu = 0.5$ for evaluation of PA gels (assuming gels are incompressible) and $\nu = 0.45$ for measurements of cortical slices (assuming cells are nearly incompressible³⁶). E is the Young's modulus, R is the radius of curvature of the indenter (i.e., the radius of the sphere; 1.25 μm), and δ is the indenter to sample distance. To solve for the Young's modulus, a maximum indentation of 500 nm was selected for fittings, since the Hertz-Sneddon model does not hold at large indentations, yet at small indentations, the Young's modulus depends significantly on the depth of indentation.⁵² Compared to the thickness of the gels (80–100 μm), 500 nm is adequately small, yet remains in the region where Young's modulus is independent of indentation depth. The data was fit from the point of contact (the point at which the derivative of the force-distance curve became nonzero) to the maximum indentation. The Young's modulus was determined for each gel using the average of all force curves.

The abovementioned methods for determining the Young's modulus of PA gels using AFM was also used to determine the Young's modulus of cortex explants. Briefly, isolated fetal rat cortices were dissected and sliced into approximately 50–150 μm long pieces. Cortex slices were plated onto a glass coverslip coated

with 100 μg/mL PDL and allowed to settle to the surface for approximately 45 min. Within this short time, attachment to the surface was minimal but precautions were taken to avoid movement of the cortices due to the AFM tip. The explants were positioned under the AFM tip as described above and force curves were taken for multiple locations for each explant. Multiple explants from three separate animals were analyzed and averaged.

Characterization of Surface-Bound Laminin

After coating glass and gel surfaces with laminin as described above, 5% of bovine serum albumin (BSA; Sigma) in PBS was applied to each substrate for 3 h. Substrates then incubated with a 1:40 dilution of primary anti-laminin (Sigma) in 3% BSA + PBS overnight at 4 °C in a humidity chamber. Gels were gently rinsed with PBS and incubated with a 1:40 dilution of secondary anti-rabbit fluorescein-linked whole antibody (GE Healthcare; Piscataway, NJ) for 3 h at 4 °C in a humidity chamber. After incubation, substrates were washed twice with PBS. Fluorescence images were taken of the substrates, with mean gray value levels quantified using ImageJ software (National Institutes of Health, Bethesda, MD). For control, PA gels without laminin-coating were immunostained as described above. Also, to verify that the amount of anti-laminin antibody was not at a saturated level, the initial amount of attached laminin was increased from 40 to 100 μg/mL and a significant increase in the fluorescence intensity was observed (data not shown).

Cell Culture and Experimental Conditions

Cortical neurons were isolated from E17 rat embryos (Taconic Farms, Hudson, NY) as described elsewhere,²⁴ with a few modifications. All experiments were carried out in accordance to protocols approved under the Institutional Animal Care and Use Committee at the University of Maryland, College Park. All chemicals and media regents were purchased from Invitrogen (Carlsbad, CA) unless otherwise specified.

In brief, neurons were isolated from cortices and dissociated with 0.25% Trypsin with EDTA for 20 min at 37 °C. Trypsin was inhibited with the addition of 1 mg/mL soybean trypsin inhibitor and cells were centrifuged for 5 min. After centrifugation, cells were resuspended in neuronal culture medium and filtered through a 70 μm cell strainer (Fischer Scientific). Neurons were grown in neuronal culture medium consisting of neurobasal medium, 2% B-27, 0.5 mM L-glutamine, 5% fetal bovine serum, and 1% penicillin/streptomycin. After 24 h, media was removed and neurons were cultured in the abovementioned neuronal

culture medium supplemented with 10 ng/mL NGF, and 10 μ M FdU and 10 μ M Uridine (Sigma-Aldrich) to prevent cell division of non-neuronal cells. Mitotic inhibitors and NGF were removed after 30 h, and cells were supplied with fresh neuronal culture medium. Dorsal root ganglion neurons were isolated from the periphery of the E17 spinal cord and cultured with the same technique described above. Here we quantify only the outgrowth lengths of single cells which lack contact to neighboring cells. This ensures that outgrowth is not influenced by factors such as cell-cell adhesion molecules or membrane-associated guidance molecules, which have regulatory roles in axon guidance and selective fasciculation.⁵⁷

All snapshots and time lapse experiments were performed using an inverted microscope (Olympus American Inc, Center Valley, PA) and a 100 W mercury lamp (Olympus). A CCD camera (Retiga SRV camera, QImaging, Surrey, BC Canada) was used for recording the images. All experiments were performed in a closed microscope chamber (Precision Plastics, Inc., Beltsville, MD) with culture conditions set at 37 °C, 5% CO₂ and 50% humidity.

Inhibition of Myosin II with Blebbistatin

Neurons were plated on laminin-coated substrates of varying stiffness. Extension behavior was observed for 30 min prior to the addition of blebbistatin (referred to as pretreatment). After 30 min, media was removed and supplemented with 25 μ M blebbistatin (Sigma-Aldrich), a myosin II inhibitor. Cells were observed for an additional 30 min. Finally, cells were rinsed and supplied with fresh media and observed for an additional 30 min (referred to as washout). Time lapse sequences were quantified with ImageJ as described in the “[Image Analysis and Statistics](#)” section.

Antibodies and Immunostaining

Specific antibodies were selected to observe the appearance of neurofilaments and dendrites during cortical outgrowth. After the specified time, cells were fixed as described elsewhere.²¹ Briefly, cells were initially rinsed with PHEM buffer. PHEM buffer was made using 60 mM PIPES, 25 mM HEPES, 10 mM 0.5 M EGTA, 2 mM MgCl₂ and sterile water, and had a final pH of approximately 7.0. After two rinses, the cells were simultaneously fixed and the membrane was extracted using 0.25% glutaraldehyde and 0.1% Triton-X-100 in PHEM buffer (referred to as FEX solution). Cells were incubated in the FEX solution for 15 min at room temperature. Cells were rinsed again twice with PHEM buffer, and then incubated in 5% BSA for 25 min at room temperature. For the

identification of neurites, primary rabbit anti-microtubule-associated protein-2 (MAP2) antibody (1:1000 dilution; Abcam, Cambridge, MA) was added to cells overnight. Cells were rinsed and then incubated in secondary anti-rabbit fluorescein-linked whole antibody (1:25 dilution, GE Healthcare) for 2 h. All incubations were performed at 4 °C in a humidity chamber. For axon specification, cells were also stained for the appearance of neurofilaments using primary mouse monoclonal (SMI31) antibody (1:1000 dilution; Abcam). Cells were incubated in the primary antibody overnight and were gently rinsed. Lastly, the secondary AlexaFluor594 goat anti-mouse antibody was added (1:200 dilution; Invitrogen) for 30 min. Cells were rinsed again and stored in PBS during observations.

Image Analysis and Statistics

Neuronal process lengths and centers of mass (in x , y coordinates) were traced by hand using ImageJ analysis software. Analysis included only those neurites which did not contact other cells or processes and were greater than 5 μ m in length. All cortical experiments were repeated in triplicate, using different E17 rat embryos for each independent experiment. ImageJ analysis was also used to identify the length of the process during extension and retraction observations, as well as blebbistatin experiments. To determine extension and retraction rates, single snapshots were taken approximately every 30 s for a total duration between 30 and 500 min, and the length of processes were measured by hand. The slope of individual extension and retraction periods were quantified and averaged for multiple cells. Data was quantified for statistical significance using either one-way ANOVA analysis or Student’s t -test. One-way ANOVA analysis was used when evaluating statistical significance among multiple groups (i.e., comparisons among stiffness), while Student’s t -test was used for determining statistical significance for single situations (i.e., comparisons of pretreatment spreading rate vs. blebbistatin-treated spreading rates).

RESULTS

Identification of Cortex Stiffness Using Atomic Force Microscopy

The majority of biological tissues and organs are soft viscoelastic materials which exhibit elastic moduli ranging on the order of 10² to 10⁵ Pa.³⁵ In order to thoroughly evaluate the effect of substrate mechanics on cortical neuron outgrowth we first determined the

native stiffness of the fetal rat cortex using atomic force microscopy (AFM). Force curve measurements were taken for multiple locations for seven separate cortex explants (see “Materials and Methods” section for determination of Young’s modulus). The average Young’s modulus for fetal rat cortex was determined as 305 ± 25 Pa (SEM). This stiffness is in the same range (263–491 Pa) of that for the swine brain predicted theoretically and supported using an *in vivo* indentation method.⁴² Quantifying the Young’s modulus of the native fetal rat cortex was critical in determining the range of polyacrylamide (PA) gel stiffness necessary to ensure observations both below and above the native environment rigidity. Thus, we decided to make gels with the range of stiffness 260 Pa–13 kPa.

Specification of Substrate Ligand Concentration and Young’s modulus

Preparation of PA gels (see “Materials and Methods” section) was performed with slight adaptations of the method described by Pelham and Wang,⁶⁰ and either a dynamic mechanical analyzer or AFM was used to determine the mechanical properties of the gels. Dynamic mechanical analysis (DMA) and AFM verified that increasing concentrations of bis-acrylamide (and acrylamide) yielded PA gels with increasing Young’s moduli. DMA resulted in gels with Young’s modulus values of 13.15 ± 2.0 kPa (8% acrylamide, 0.2% bis, as previously reported⁵⁶), 986 ± 140 Pa (3% acrylamide, 0.2% bis), and 867 ± 180 Pa (3% acrylamide, 0.1% bis). AFM resulted in gels with Young’s modulus values of 422 ± 6 Pa (3% acrylamide, 0.06% bis) and 260 ± 2 Pa (3% acrylamide, 0.04% bis).

To ensure that observed neurite outgrowth dynamics and behavior result from substrate stiffness and not the concentration of adhesive ligand, the concentration of laminin was adjusted for glass coated substrates such that the differences between the gels and glass were not significant. To do so, substrates were incubated with $40 \mu\text{g}/\text{mL}$ of laminin and anti-laminin antibodies were used to identify the intensity of laminin present on the substrate surface (see “Materials and Methods” section for more details). Epifluorescence snapshots were captured for 5–12 locations on each gel and the mean gray value was determined using ImageJ. The arbitrary fluorescence intensity values were similar for all gel substrates, and only glass illustrated a significantly increased concentration of laminin (Fig. 1). Laminin titrations were created to determine the necessary amount of protein required on the glass surface to compliment the concentration present on the gel surfaces (Fig. 1b). Therefore, to reach similar protein content, $5 \mu\text{g}/\text{mL}$

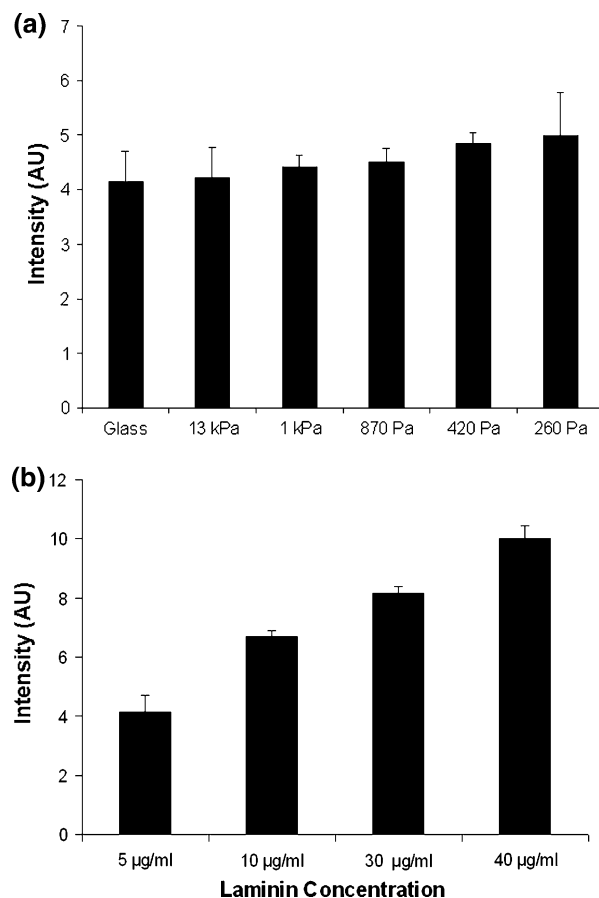


FIGURE 1. Specification of ligand concentration was determined by adding fluorescently labeled anti-laminin antibody to laminin-coated substrates. Epifluorescence snapshots were captured for each gel with the average mean gray value displayed. The arbitrary fluorescence intensity values were similar for all gel substrates when incubated with $40 \mu\text{g}/\text{mL}$ of laminin; however the intensity was significantly increased on glass substrates (a). Laminin titrations were performed to determine the approximate amount of laminin protein required on the glass surface to compliment the concentration present on the gels (b). To minimize effects from ligand concentration, $5 \mu\text{g}/\text{mL}$ laminin was added to glass substrates, while $40 \mu\text{g}/\text{mL}$ was added to PA gels to reach similar fluorescence intensities (as shown in (a)), after which no differences among intensities are reported. Error bars represent standard error.

laminin was added to glass substrates, while $40 \mu\text{g}/\text{mL}$ was added to PA gels (Fig. 1). Typically, gels of similar acrylamide concentration do not vary in the amount of present surface ligand,^{37,47,48,56} therefore it was not unexpected that all gels of 3% acrylamide (and varying percentages of bisacrylamide) were similar in intensity. It is also not entirely unusual that we did not see a significant increase in the amount of ligand present on the 8% acrylamide, 0.2% bisacrylamide, since others have shown similar ligand concentrations between polyacrylamide gels with a 6% difference in acrylamide percentages.³³ Correcting for the concentration of ligand present on the surface ensures that differences in

cellular behavior are due to mechanical differences and not the concentration of surface ligand. Although we were unable to qualitatively determine the amount of PDL on the substrates due to a lack of comparable fluorescent tags, we suspect that gels will have similar expression on their surface after coating, as seen with laminin. We also coated glass coverslips with varying concentration of PDL, 10, 50, or 100 $\mu\text{g}/\text{mL}$ PDL, and observed no significant differences in the length of the longest process (data not shown).

Axonal Differentiation of Cortical Neurons is Insensitive to Substrate Stiffness

Although a significant amount of work has been recently performed on the effect of substrate compliance on neurite outgrowth for spinal cord,¹⁸ DRG,^{2,62} hippocampal³¹ and PC12 cells,³³ less work exists on the mechanosensitive properties of cortical neurons. Recently, Georges *et al.*²² has reported similar lengths in process outgrowth for cortical neurons plated onto substrates of varying stiffness; however, this study used neuron and glial co-cultures which were observed after 6 days. After this length of time, dissociated cortices were abundant on both soft and hard substrates and were densely packed with multiple processes connecting.²² It is possible that this cell–cell contact and synapse formation can alter the behavior of neurons, since outgrowth can be influenced by cell–cell adhesion molecules and membrane-associated guidance molecules,^{1,57} and spontaneous synapse connections and current can be detected as early as 4 days in culture.³ Here we hypothesized that if cortical neurons were sensitive to substrate stiffness then the differences in outgrowth behavior would most likely be observed during the first 72 h or even during bursts of growth and retraction, when axons differentiate. To investigate the effects of substrate stiffness on cortical neuron differentiation, cortices were isolated, dissociated and plated onto laminin or PDL substrates and cultured for 72 h.

To qualitatively determine when axons are specified, cells were fixed at 6, 24, 48, and 72 h and were then stained with MAP2 to stain the microtubule associated proteins in neurites, and SMI31 to stain the neurofilaments (NF) present only in the axon of each cell (Fig. 2). Among stiffness and protein coating, we notice similar staining presence during the course of the 72 h observed. After 6 h, small neurites are present, as identified in green with the MAP2 antibody. No SMI31 (red) staining is present in the processes, illustrating that no NF are present in any of the processes, and thus no neurites have differentiated into axons. After 24 h, however, some cells stain positive for neurofilaments, although the stain is typically weak in

expression and is not present in the majority of cells. The most noticeable NF staining occurs at the 48 h time point, where neurites are clearly stained green and one process is positively stained red for the presence of NF. After 72 h, this becomes even more noticeable. Overall, this suggests that cortical neurons begin differentiating after the addition of NGF (24–48 h) and the most apparent NF positive staining occurs at 72 h when the axon is clearly specified. It is not surprising that the time at which axons begin to differentiate corresponds to the time at which NGF is added to the media, since NGF encourages differentiation of many cell types^{25,58} and is required for nerve growth during development.⁵⁹ However, what is surprising is that differentiation occurs regardless of substrate stiffness.

To quantitatively confirm these observations, we used the three-stage process of differentiation originally described by Dottie *et al.*¹⁴ and also used by others.³¹ Neurons were classified as Stage 1 when there was an absence of neurites. For us, the majority of Stage 1 neurons were observed around 6 h of plating. Stage 2 was used to classify neurons where the neurites were similar in length. Typically, these cells did not stain for SMI31. Lastly, neurons were classified as Stage 3 when a significantly long axon emerged and stained positive for SMI31, indicating that this process is indeed an axon. The majority of Stage 3 neurons were observed between 48 and 72 h. The percentage of cells in Stage 3 from 24 to 72 h is displayed in Fig. 2 for laminin (Fig. 2c) and PDL-coated (Fig. 2d) substrates. For laminin, differentiation occurred for 40–50% of cells at 24 h, 50–60% of cells at 48 h and 70–80% of cells at 72 h. Similarly, for PDL, differentiation occurred for 40–50% of cells at 24 h, 60–70% of cells at 48 h and 75–85% of cells at 72 h. Overall, the percentage of neurons classified as Stage 3 increased during this time period, however, unlike hippocampal neurons where more Stage 3 neurons are observed on soft substrates,³¹ for cortical neurons we did not observe a trend among stiffnesses for either protein coating. This illustrates that cortical neuron differentiation is insensitive to matrix compliance and protein coating.

Cortical Outgrowth is Insensitive to Substrate Stiffness

The length of the longest process during differentiation has long been used as a method to distinguish axons vs. dendrites and to classify cells as Stage 3 neurons.¹² Although we illustrate above that axons differentiate similarly regardless of substrate compliance, it remains unknown whether the axons also extend to similar lengths during this differentiation process. To quantify the length of axons during extension, snapshots were captured at 6, 24, 48, and

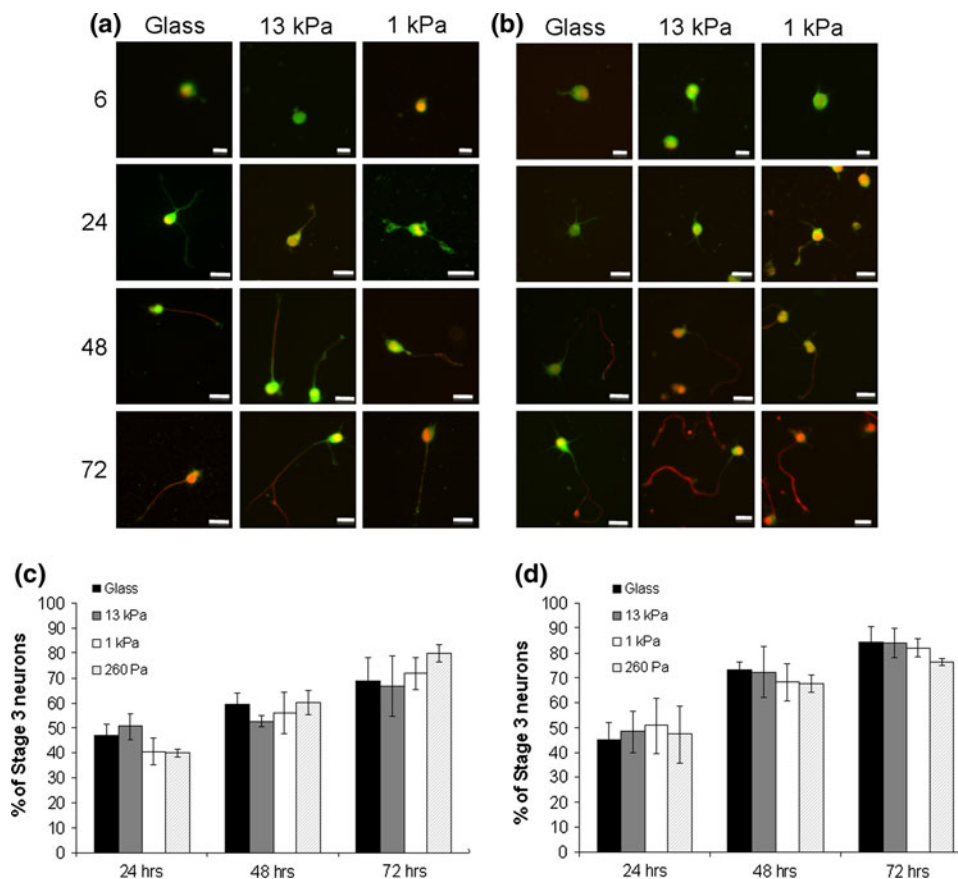


FIGURE 2. Cortical neurons exhibit similar differentiation behavior regardless of stiffness. Cells were fixed at 6, 24, 48, and 72 h after plating on laminin (a) and poly-D-lysine (PDL; b) coated substrates of varying stiffness. Cells were stained with MAP2 (green) to identify microtubule associated proteins in neurites, and SMI31 (red) to identify neurofilaments (NF) present only in the axon of each cell. Overall, a similar staining presence is observed during the course of the observed 72 h. At 6 h, small neurites are present, and stain positive for MAP2, but not SMI31. After 24 h, some cells express positive staining for SMI31, however the majority of the cells only express MAP2 staining. At 48 h, more noticeable NF localization occurs, with the strong identification of red axons most apparent after 72 h. Cells were classified as Stage 1, 2, or 3 neurons for laminin (c) and PDL-coated (d) substrates. Stage 3 neurons refer to those cells with specified axons (positive staining for SMI31 in one process). No significant differences are observed among substrate compliance for either protein coating (using one-way ANOVA analysis, $p > 0.05$), illustrating that cortical neurons differentiate independently of substrate stiffness. Error bars represent standard error.

72 h post plating and images were analyzed for the number of neurites and individual neurite lengths. The average length of the longest process for each neuron is displayed in Fig. 3 for both laminin and PDL coated substrates. Interestingly, after 72 h, we did not see statistically significant substrate-dependent differences in the length of the longest process for either protein coating (using one-way ANOVA analysis, $p > 0.05$). This data shows that cortical neurons are capable of extending processes of similar lengths regardless of the substrate compliance for both integrin-mediated (laminin coating) and non-integrin-mediated adhesion (PDL coating). When comparing the length of the longest process to the second longest process, this ratio was also similar for all stiffness. The longest process was on average 3–5 times the length of the second longest process at 48 and 72 h for both laminin and

PDL substrates (data not shown). This emphasizes that the longest process is many times longer than the other neurites, which has been also used as a method to classify neurons as Stage 3 and to distinguish an axon vs. dendrite, and is consistent with our differentiation observations.¹² From this, one can also conclude that at 72 h, the longest process, which is typically 90–120 μm in length is indeed the axon, since the majority of cells at this time point (approximately 80%, see Fig. 2) have differentiated. In addition to the longest process per cell, substrate stiffness did not affect the average number of processes per cell (Figs. 3b and 3e), unlike others³³ who see increased neurites for PC12s plated on stiffer substrates. Also, we observe no substrate affects on the average length of all processes per cell (Figs. 3c and 3f) after 72 h of culture (using one-way ANOVA analysis, $p > 0.05$).

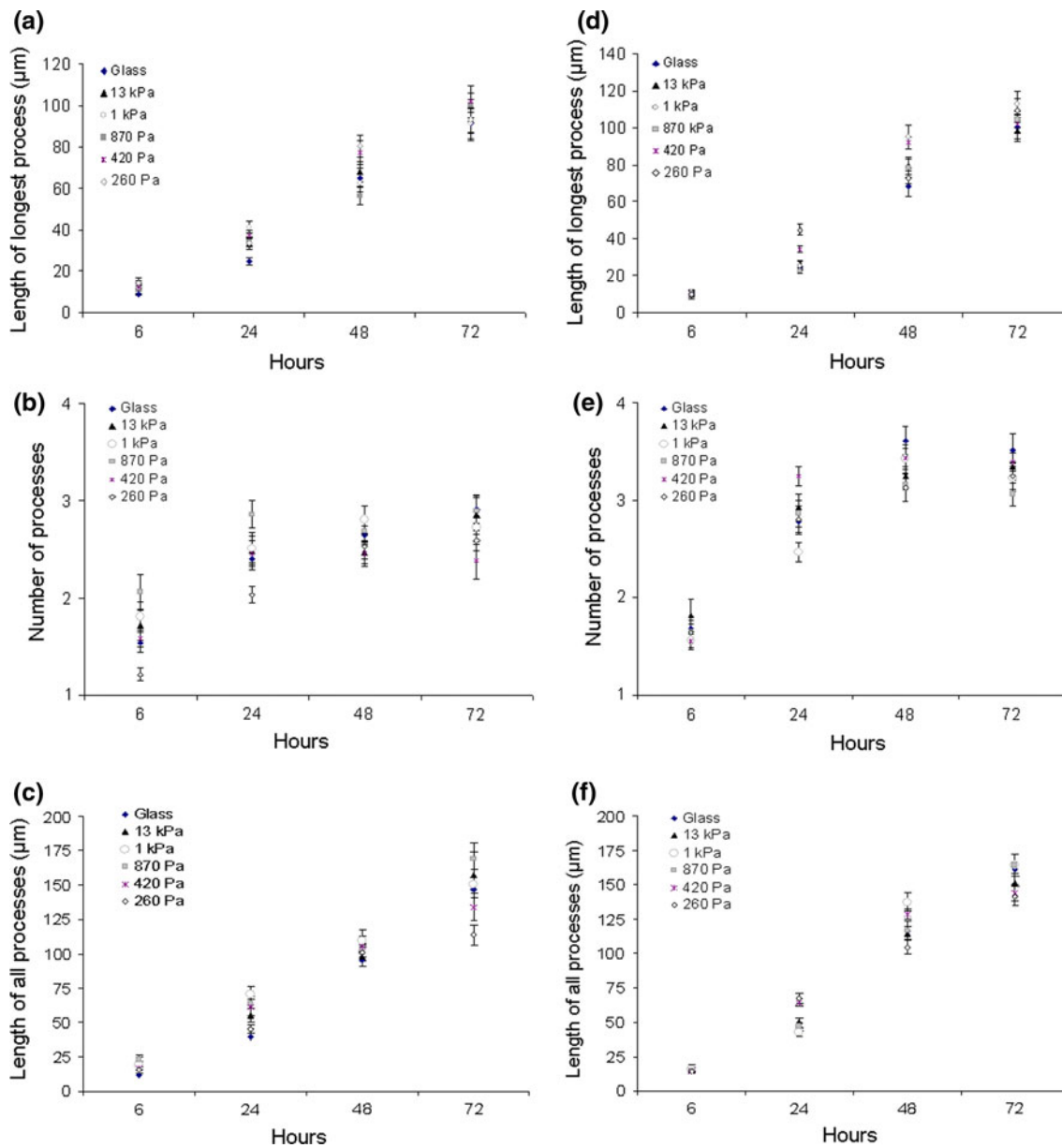


FIGURE 3. Cortical neuron outgrowth was observed for cells plated onto substrates of varying stiffness. Cells were plated onto laminin (a–c) or PDL (d–f) substrates. The average length for the longest process (a and d), average number of processes (b and e) and the average length of all processes (c and f) per cell illustrate similar behavior regardless of substrate stiffness for both laminin and PDL substrates. All parameters illustrate no statistically significant differences after 72 h (using one-way ANOVA analysis, $p > 0.05$). (For all cases, error bars represent standard error and $N = 30-60$ cells).

Although Fig. 3 may suggest that neurite and axon extension is a linear phenomenon, it is known that this is not the case.^{13,45} Rather than extending a continuous process slowly over the course of 72 h, axons actually exhibit periods of extension, retraction and stalling. One explanation for the lack of difference in process lengths at the observed time points is the possibility that neurons extend processes at different rates on different stiffnesses. For example, it may be possible that differences in extension and retraction rates are

occurring; however this dynamics is not observed when single snapshots are recorded at each time point. To further evaluate this possibility, we observed individual neurites during outgrowth using time lapse microscopy. Snapshots of individual neurites were taken every 30 s for a period of observation ranging from 30 to 500 min for soft (260 and 870 Pa) intermediate (13 kPa) and stiff (glass) substrates. Neurite lengths were traced and the rate of individual periods of extension and retraction were quantified (Fig. 4).

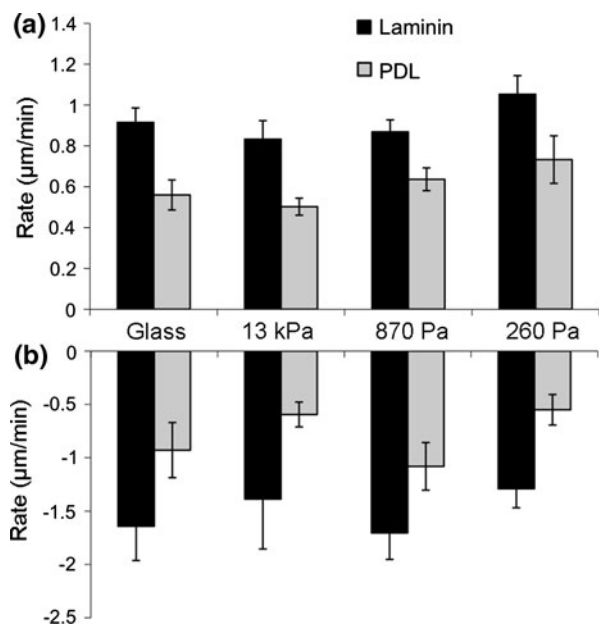


FIGURE 4. Axon extension and retraction dynamics for laminin and PDL-coated substrates. The average rate of process extension for laminin and PDL-coated substrates (a). For extension, $N = 59, 67, 61,$ and 43 for laminin coated glass, 13 kPa, 870 Pa and 260 Pa, respectively, while $N = 38, 58, 45,$ and 22 for PDL-coated substrates. The average retraction rate for laminin and PDL-coated substrates (b). For retraction, $N = 23, 22, 22,$ and 29 for laminin coated glass, 13 kPa, 870 Pa and 260 Pa, respectively, while $N = 7, 14, 15,$ and 12 for PDL-coated substrates. Overall, both extension and retraction rates occur independently of substrate modulus for both laminin and PDL-coated substrates, with no significant differences occurring among stiffnesses (using one-way ANOVA analysis, $p > 0.05$). Error bars represent standard error.

Interestingly, for laminin-coated substrates, there were no significant differences (one-way ANOVA analysis, $p > 0.05$) in the rate of extension on glass ($0.92 \pm 0.07 \mu\text{m}/\text{min}$; $N = 59$), 13 kPa ($0.83 \pm 0.09 \mu\text{m}/\text{min}$, $N = 67$), 870 Pa ($0.87 \pm 0.06 \mu\text{m}/\text{min}$, $N = 61$), or 260 Pa ($1.05 \pm 0.1, N = 43$) substrates. The rate of extension on PDL-coated substrates was significantly reduced on all substrates compared to laminin, similar in behavior to retinal explants.³⁴ However, as seen with laminin substrates, there were no significant differences among glass ($0.56 \pm 0.07 \mu\text{m}/\text{min}$; $N = 38$), 13 kPa ($0.50 \pm 0.04 \mu\text{m}/\text{min}$, $N = 58$), 870 Pa ($0.64 \pm 0.06 \mu\text{m}/\text{min}$, $N = 45$), or 260 Pa ($0.73 \pm 0.12 \mu\text{m}/\text{min}$, $N = 22$) PDL substrates. There were also no significant differences (one-way ANOVA analysis, $p > 0.05$) in the rate of retraction on glass ($-1.64 \pm 0.32 \mu\text{m}/\text{min}$; $N = 23$), 13 kPa ($-1.39 \pm 0.47 \mu\text{m}/\text{min}$, $N = 22$), 870 Pa ($-1.70 \pm 0.25 \mu\text{m}/\text{min}$, $N = 22$), or 260 Pa ($-1.30 \pm 0.18, N = 19$) laminin substrates. As with extension, the rate of retraction on PDL-coated substrates was also statistically reduced on all substrates compared to laminin. Yet, again as seen with laminin substrates,

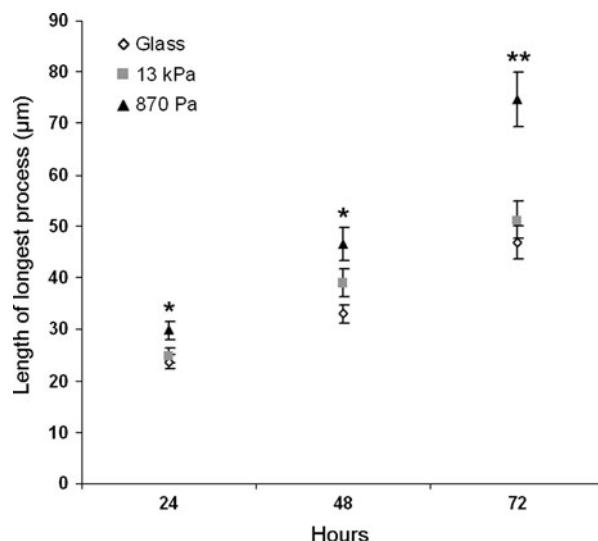


FIGURE 5. Dorsal root ganglion (DRG) outgrowth on substrates of varying stiffness. Dissociated DRG neurons were plated onto stiff (glass), intermediate (13 kPa) and soft (870 Pa) PDL-coated substrates. The average length of the longest process per cell is reported at $24, 48$ and 72 h of culture. At all time points, process extension is statistically increased on 870 Pa PA gels compared to both glass and 13 kPa substrates (using Student's t -test, $p < 0.05$ (single asterisk) and $p < 0.01$ (double asterisk), $N = 30$ – 50 neurons per time point). Error bars represent standard error.

there were no significant differences among retraction dynamics on glass ($-0.93 \pm 0.26 \mu\text{m}/\text{min}$; $N = 7$), 13 kPa ($-0.59 \pm 0.12 \mu\text{m}/\text{min}$, $N = 14$), 870 Pa ($-1.08 \pm 0.22 \mu\text{m}/\text{min}$, $N = 15$), or 260 Pa ($-0.55 \pm 0.14 \mu\text{m}/\text{min}$, $N = 12$) PDL substrates.

To further verify that the PA gel system which we are using in this study is appropriate for mechanosensitive neurons, we observed the outgrowth behavior of dorsal root ganglion (DRG) neurons. Because increased neurite outgrowth on softer substrates has been illustrated for DRGs in 3D gels,^{2,62} we suspected that we should also see a significant increase in the extension of DRG processes when plated onto PA gels of varying stiffness. DRGs were isolated from E17 rat pups, dissociated, and plated onto PDL coated substrates. Cells were plated onto stiff (glass), intermediate (13 kPa) and soft (870 Pa) substrates and snapshots were captured after $24, 48$ and 72 h of culture (Fig. 5). Based on previous investigations of DRG outgrowth which report differences with stiffness,^{2,62} we suspect that this selected stiffness range is appropriate to observe substrate-dependent affects and is also physiologically relevant based on measurements of spinal cord and brain.^{15,17,41,49} This stiffness range also allowed us to compare mechanotactic behavior of DRG vs. cortical neurons. Processes were observed on all substrates, however, the longest processes were present on the softest (870 Pa) gel. Process extension

on the softest gel was statistically increased compared to both the stiff and intermediate stiffnesses at all observed time points. This data illustrates that similarly to that reported with 3D gels,^{2,62} DRG neurons retain their mechanosensitive properties on 2D PA gels.

Process Extension is more Directed on Laminin-Coated Substrates

Although the average length of the longest process was comparable between laminin and PDL-coated substrates after 72 h (Fig. 3), differences in extension morphology were apparent (Figs. 2a, 2b and 6b). The differences in process extension were most noticeable at 72 h, when the longest process had extended to approximately 90–120 μm in length. To quantify the differences in extension, we defined a persistence index (or tortuosity) for each condition calculated by measuring the contour length, L_C and the “end-to-end” outgrowth length, L_S . The schematic shown in Fig. 6a illustrates these two parameters. When the ratio of

$L_C/L_S = 1$, the process is perfectly straight. Increased tortuosity is represented by an increase in L_C/L_S . For all compliances, cells on PDL coated substrates had a significantly increased persistence index, illustrating that they were more meandering during outgrowth compared to laminin-coated substrates (Fig. 6c). Also, when plated at a higher concentration, aggregated cells extended differently on laminin vs. PDL. On PDL, neurons aggregated into a more interwoven pattern, with processes extending in an undirected manner (data not show), similar to that described by Lemmon *et al.*³⁴ When neurons were plated at a higher concentration on laminin, aggregation was still observed but processes were more aligned on top of each other and extended more directly from aggregated groups. Meandering processes may serve as a method for the axon to find synaptic targets that it wouldn't necessarily encounter if extending with a straight trajectory and has therefore been suggested as a possible mechanisms to search for specific targets.²⁹ Extension and retraction behavior as well as adhesion likely contribute to this increase in tortuosity on PDL substrates.

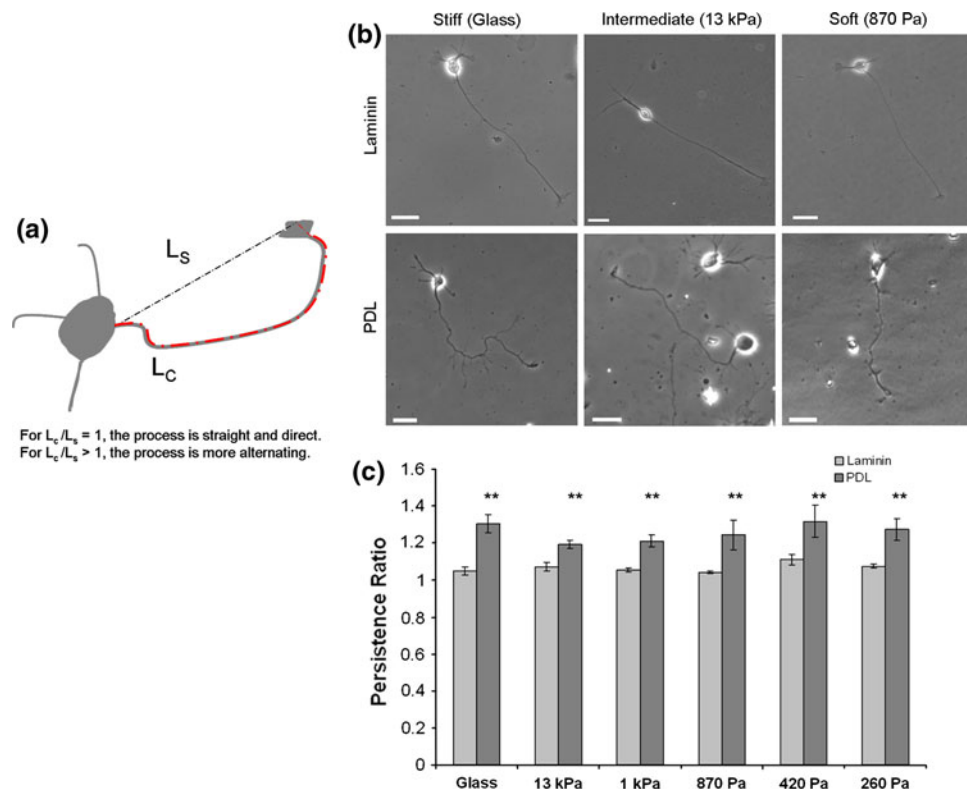


FIGURE 6. Process extension occurs differently on laminin vs. PDL-coated substrates. Schematic representation of persistence measurements (a). To quantify extension, we define an average persistence index (L_C/L_S) for each condition, calculated by first measuring the contour length (red line), followed by the straight outgrowth length (black line). If $L_C/L_S = 1$, the process is directed and straight, $L_C/L_S > 1$ identifies processes which are less directed. Representative images are shown after 72 h for soft (870 Pa), intermediate (13 kPa), and stiff (glass) substrates (b). Noticeable differences in directionality are observed between PDL and laminin. Scale bar is 25 μm in all images. Quantified data illustrates that all processes extending from PDL coated surfaces are less persistent (higher ratio) (c). Asterisks denote statistical significance (Student's *t*-test, $p < 0.01$). Error bars represent standard error.

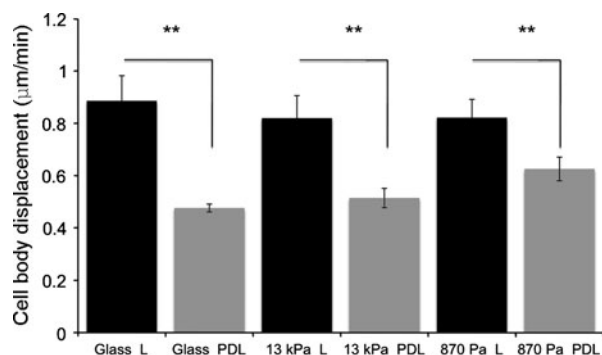


FIGURE 7. Cell body displacements are increased on laminin-coated substrates. Mean squared displacements (MSD) were calculated for 10–15 cells. Neurons cultured on laminin-coated substrates (“L”) exhibit significantly larger cell body displacements during axon extension compared to those cultured on PDL (Student’s *t*-test, $p < 0.01$). Error bars represent standard error.

In addition to the observed difference in axon extension morphology, the amount of cell body movement during the initial stages of process outgrowth was also noticeably different between PDL and laminin-coated. Cells were observed before a long process had differentiated, since this was the period where the most displacement was noticed. To quantify cell body displacements, the center of mass of the cell body (in x, y coordinates) was tracked for each frame of the time lapse sequence (30 min sequence with 1 frame per 30 s) using ImageJ tracing tools. Mean squared displacements (MSD) were calculated for 10–15 cells with the averages plotted in Fig. 7. Overall, cell–body displacement was independent of stiffness, although neurons cultured on laminin-coated substrates exhibited statistically larger cell body displacements during axon extension compared to those cultured on PDL. Note, however, that is difficult to directly compare the two different protein coatings because laminin is an integrin-based adhesion and PDL involves electrostatic (or integrin independent) interactions. The decrease in cell body movement is likely caused by an increase in cell–substrate adhesion, which has been reported for polylysine.²⁷ The decrease in extension rate for processes extending on PDL vs. laminin-coated substrates also supports this increase in adhesiveness (Fig. 4).

It is important to note that although neurons plated onto both laminin and PDL exhibit some degree of cell body displacement, the magnitude of these displacements may contribute to the measurements of the longest process between 6 and 72 h (Figs. 3a and 3d). Since the cell body displaces more on laminin substrates, it is possible that this could cause axons to be shorter in length, since if the cell body moves in the direction of the growth cone, this would reduce the

length between cell body and the tip of the longest process. This may be a reason why process extension length on laminin-coated substrates is similar to PDL substrates during the first 72 h of culture (Figs. 3a and 3d). Although it is impossible to distinguish from snapshots whether the cell body has recently displaced, using time lapse microscopy we were able to determine these precise events and ensured that they did not contribute to the retraction or extension speeds reported in Fig. 4. Extension was considered only if the growth cone itself was moving forward, while retraction was considered only if the growth cone moved towards the cell body.

Myosin II Inhibition is Independent of Substrate Stiffness

Myosin II (MII) is a motor protein that, in combination with actin, can generate cellular contractile forces and is required for growth cone motility.⁷ Recent focus on the role of MII (as well as other isoforms) has shown implications of myosin in both the extension and retraction phases of axon development. For example, down-regulation of MIIA and MIIB has illustrated an inhibition of neurite extension in N2A cells,⁶⁴ and the protrusion of filopodia (an essential step in growth cone advancement⁴) requires myosin activity.⁷ Myosins are also implicated in axon retraction. For instance, axon retraction was prevented by the inhibition of MII for sever-induced axons,²⁰ as well as for established axons *in vivo* following negative regulation of RhoA or ROCK.⁵ More recently, it has been suggested that MII functions in a substratum-dependent manner.³⁰ Although Ketschek *et al.*³⁰ report differences in myosin inhibition for cells extending on laminin vs. lysine, the role of MII during axon extension on substrates of varying compliance remains unknown. Because rigidity sensing has been shown to be integrin-dependent,^{28,31} we evaluate how MII inhibition affects both the extension phase as well as the stalled phase of axon outgrowth on laminin-coated surfaces of varying stiffness. We hypothesized that if cortical neuron extension is independent of substrate stiffness, then the inhibition of MII should affect axons similarly regardless of substrate compliance.

To test the effects of MII inhibition on axon extension, time lapse sequences were taken for individual processes for 30 min prior to treatment (pretreatment). After 30 min, 25 μ M blebbistatin was added and processes were observed for an additional 30 min. Lastly, the blebbistatin solution was removed and fresh media was added while extension was observed for an additional 30 min (washout). The length of extension over the course of this 90 min period was quantified using ImageJ (see: “[Materials and Methods](#)” section for a

detailed explanation). Cells were classified as either “extending” or “stalled” based on the rate of the first 30 min of observation, prior to the addition of blebbistatin. “Extending processes” were those which were increasing in length with a speed $\geq 0.2 \mu\text{m}/\text{min}$, while those considered “stalled processes” exhibited little or no extension with rates between -0.15 and $0.2 \mu\text{m}/\text{min}$. The average rate of extension during pretreatment as well as blebbistatin treatment is displayed in Fig. 8. The rates of extension during the washout period were comparable to that of the pretreatment rates (data not shown). MII inhibition caused no significant differences in the extension rate of previously extending axons for all laminin-coated substrates. Although the extension rate during blebbistatin treatment on glass appears larger (Fig. 8), there were no significant differences between the speeds during blebbistatin

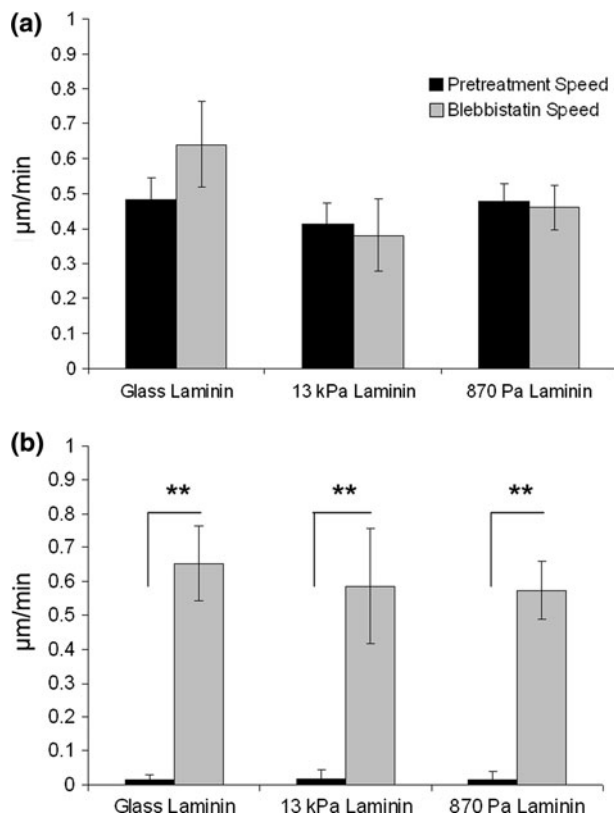


FIGURE 8. Inhibition of myosin II with blebbistatin identifies extension dependent effects. Neurons plated onto laminin coated substrates were affected by blebbistatin similarly regardless of substrate stiffness, but dependent on extension behavior. MII inhibition caused no significant differences ($p > 0.05$, using Student’s *t*-test) in the extension rate of previously extending axons for all laminin coated substrates (a). Also, there were no significant differences between the speeds during blebbistatin treatment between laminin-coated substrates of varying stiffness. When cells are initially in a stalled state, the inhibition of MII causes a statistically significant increase (asterisk denotes statistical significant using Student’s *t*-test with $p < 0.01$) in extension regardless of substrate stiffness (b). Error bars represent standard error.

treatment among laminin-coated substrates of varying stiffness. Unlike Ketschek *et al.*,³⁰ we do not see a decrease in the rate of extension during blebbistatin treatment of laminin-coated glass. These discrepancies could be due to differences in laminin concentration ($25 \mu\text{g}/\text{mL}$ ³⁰ vs. $5 \mu\text{g}/\text{mL}$), type of neurons (E7 chicken DRGs vs. cortical neurons), and dissociated single cells vs. cultured explants.³⁰ We also note that the pretreatment rate for laminin is slightly reduced compared to that reported in Fig. 4, however these rates are not significantly different and remain within one standard deviation from the mean.

Most interestingly, we report statistically significant increases in the speed of extension when MII is inhibited during a stalled period of axon development regardless of substrate stiffness (Fig. 8b). As seen with axons which were initially extending, there are no significant differences between the extension rates during blebbistatin treatment for laminin, illustrating again that this is not dependent on substrate stiffness. Collectively, this data illustrates that MII does not appear to be regulated differently on different stiffnesses, and also suggests MII inhibition as a method to encourage axon outgrowth when processes were previously in a stalled period of growth.

DISCUSSION

Dramatic changes in the mechanical environment of various organs and tissues have been associated with both disease and injury. With respect to the nervous system, a focus on the mechanical changes occurring following spinal cord injury and traumatic brain injury has been of much current interest.⁴³ Recent work has illustrated that the hippocampus is a mechanically heterogeneous environment, possessing regions of varying elastic moduli¹⁵ and differences in the viscoelastic properties of neuron vs. non-neuronal cell populations.³⁸ Due to the differences in the mechanical environment of the hippocampus, it is not surprising that isolated hippocampal neurons are mechanosensitive, growing preferentially on softer substrates.³¹ Here, we show that, unlike DRG (Fig. 5) and hippocampal neurons,³¹ cortical neurons appear to be insensitive to the substrate stiffness. We report not only similar times of differentiation (Fig. 2), but also similar behavior in process length and number (Fig. 3), extension and retraction dynamics (Fig. 4), and myosin activity (Fig. 8). The ability of cortical neurons to extend long processes on substrates with varying stiffness is not entirely surprising, as others have briefly mentioned this phenomenon,²² although they do not consider extension and retraction behavior. This behavior does contrast with that of hippocampal³¹ and

spinal cord¹⁸ neurons which exhibit more neuron-like behavior on softer substrates. However, as previously mentioned, differences in the age and class of neurons, cell density, time and length of observation, dimensionality, ligand selection and concentration and media conditions are just some variables which may contribute to differences in observed behaviors.

Various cell types subjected to mechanical stimuli *in vivo*, including epithelial,⁴⁷ neutrophils,⁵⁶ endothelial,⁶⁵ fibroblasts^{47,65} and stem cells^{16,53,54} have all been shown to respond to the mechanical properties of their environment whether in changes in morphology, migration or differentiation. In the brain, however, cortical neurons do not generally bear significant load and are secluded to their environment due to their discrete localization. We suspect that the insensitivity to substrate stiffness which we report here may arise due to the native properties of the fetal rat cortex during the selected stage of development. During corticogenesis, neurons exhibit radial migration, starting from the ventricular zone and ending up in one of the six layers of the cortex.⁵⁰ The development of these cortical layers occurs throughout the last weeks of gestation for the fetal rat. In particular, layer VI, the deepest and innermost neuron layer, is generated between E13 and E16, while layer II/III neurons are not produced until the very end of the gestation period, around E18–E21.²⁴ The higher the cortical layer, the closer to the ventricular zone the neurons are, illustrating that the neurons are reaching final cortical development at the end of gestation when layers II and III are formed. Like others, we isolate cortical neurons from E17 fetal rats due to the maximal proliferation of neurons at this date.²⁴ It is possible that the migration of these neurons *in vivo* is independent of substrate stiffness, since the signaling required to order cortical neurons into distinct layers appears more chemical in nature and is reliant on the presence of the glycoprotein Reelin.⁵¹ Due to the very soft nature of the cortex during this stage of development, we were not able to isolate separate layers of the cortex in order to determine the stiffness of each cortical layer; however, as described above, we did probe various random slices of the cortex and found a similar stiffness ($E = 305 \pm 25$ Pa) for each tested sample. Collectively, the data we present here suggest that, during this early stage of development, there are no discernible differences in stiffness in the cortex. This mechanical homogeneity of the cortex may contribute to the inability of cortical neurons to sense stiffness at this stage of development. It would be interesting to determine whether this homogeneity is retained throughout the rest of fetal and neonatal development. Alternatively, if subtle stiffness changes are present in the cortex during development, but not detected using

AFM, it is possible that the ability of cortical neurons to differentiate similarly on substrates of varying compliance (Fig. 2) (compared to hippocampal neurons, which differentiate axons more readily on softer substrates³¹) may serve as a strategy during the development of the distinct cortical layers.

Further evaluation of the local structure of brain tissue in the cortex would be of potential interest to better understand why the mechanosensitivity of cortical neurons varies from other locals, such as the hippocampus. Since it has previously been shown that protein expression can regulate the response of rigidity sensing mechanisms in hippocampal neurons,³¹ it is likely that the protein expression within the cortex is contributing to the rigidity response of cortical neurons as well. In fact, the rigidity sensing mechanisms and response of hippocampal neurons to fibronectin vs. laminin-coated substrates vary.³¹ Therefore, the presentation and expression of both chemical and mechanical differences in the brain tissue can influence the mechanosensitive behavior of neuronal populations, and likely differs among location within the nervous system.

One might initially suspect that the length of processes on PDL-coated substrates should be reduced compared to laminin, since the individual extension rate was significantly increased on laminin-coated substrates (Fig. 4). However, although axon extension on laminin substrates is increased, the retraction rate is also significantly larger than on PDL substrates. In addition, for individual extension and retraction events, the average duration of extension was longer for PDL substrates, while the average duration of retraction was shorter. Characteristic examples of axon extension on glass coated with laminin and PDL are shown in Fig. 9a. The difference in outgrowth dynamics is very clear, with laminin-coated substrates illustrating many more periods of rapid retraction and extension. In certain cases, rapid retraction may cause sharp movement of the cell body, displacing it towards the growth cone. Again, these events are not included in average retraction rates; however, they are present more frequently on laminin-coated substrates and do contribute to the overall effect on length. Alternatively, the growth cone also exhibits rapid retraction events, such as that marked with a cross in Fig. 9a, and illustrated in Fig. 9b. This decrease of approximately $30 \mu\text{m}$ occurs over the course of 2 min and is interestingly comparable to the rate of microtubule depolymerization, which occurs between 20 and $30 \mu\text{m}/\text{min}$.⁶ Other retraction events (such as that marked with an asterisk in Fig. 9a) occur more slowly, with an average rate of approximately $-1.64 \mu\text{m}/\text{min}$ for laminin-coated glass, and are likely caused by a combination of acto-myosin contraction,

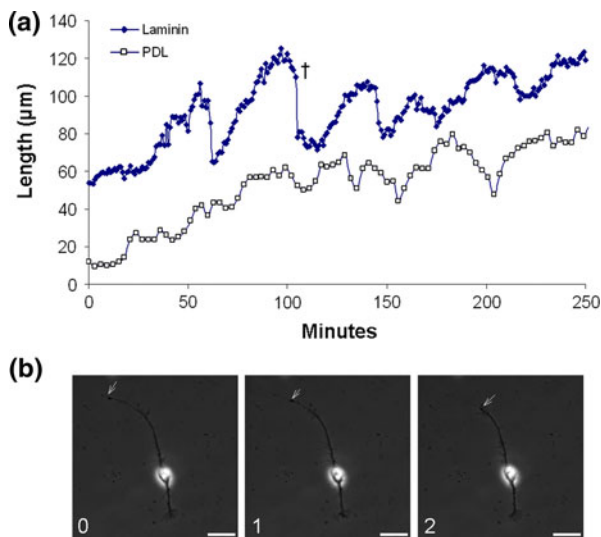


FIGURE 9. Long-term observations of axon outgrowth between 49 and 53 h of culture on laminin and PDL-coated glass substrates reveal numerous periods of extension, retraction and stalling (a). Note the laminin curve is displaced up $25 \mu\text{m}$ for clarity. The frequency of retraction events is increased for laminin substrates. An example of rapid retraction of the growth cone (marked by a cross in (a)) is illustrated in (b). A reduction in approximately $30 \mu\text{m}$ occurs over the course of 2 min (time marked in lower left corner), while less dramatic retraction events are also observed (marked with an asterisk in (a)). This figure illustrates the increased duration of extension periods on PDL substrates and also highlights both the increased extension and retraction rates on laminin substrates. Scale bar is $25 \mu\text{m}$.

traction stresses and cell tension, which we further address below.

Initially, it was surprising that neurons plated on different compliances extend and retract with similar rates, considering Franze *et al.*¹⁹ have recently illustrated that neurons retract when stress applied to the growth cones of cortical neurons is increased. In their work, Franze *et al.* applied a mechanical stress to the tip of PC12 growth cones and reported a retraction threshold ($274 \pm 41 \text{ pN}/\mu\text{m}^2$). Below this level growth cone protrusion is not disturbed, yet above this level growth cones retract. From this, we suspected that we may see differences in the retraction behavior for cells plated onto our softest gels (260 Pa) compared to more stiff substrates. However, as shown in Fig. 4, we observe similar retraction (and extension) behavior regardless of stiffness. Even more, during the stalling periods actomyosin and traction forces dominate the dynamics of the growth cone, if there were any differences due to stiffness we should have seen different outgrowth upon MII inhibition, however we observe the same rate of growth in all stiffness tested. This leads us to believe that, because cortical neurons appear to have all the basic machinery necessary to sense substrate stiffness (including myosin, actin, and

cell-substrate adhesions) according to the motor-clutch dynamics model,⁹ we suspect that cortical neurons may lack or down-regulate some form of rigidity-sensing mechanisms such as receptor-like protein tyrosine phosphatase α (RPTP α), which is required for mechanosensing in hippocampal neurons,³¹ or potentially a yet unidentified mechanotactic protein.

An additionally valuable result from this work is the identification that myosin II inhibition during a previously stalled stage of axon outgrowth encourages axon extension for all laminin-coated substrates (Fig. 8). The effects on outgrowth which we observe following MII inhibition can be explained by the forces involved in axon outgrowth. A simplified schematic of the cytoskeletal components and forces involved in extension/retraction events are illustrated in Fig. 10. Axon outgrowth requires a driving polymerization force at the tip of the growth cone F_p , which is balanced by extracellular matrix (ECM) adhesion, using integrins. These integrin based adhesions have been associated with the rigidity sensing of both neuronal³¹ and non-neuronal cell types²⁸ and create traction force coupled with the substrate, F_s . An additional force, F_m , present during axon extension arises from actomyosin contractility. Actomyosin forces arise from the contractility of myosin subunits on actin bundles, and the “pulling” of these actomyosin complexes contribute to forward movement.³² Overall, an appropriate balance between F-actin turnover and actomyosin contractility is necessary for the maintenance of proper mechanical tension⁵⁵ and axonal outgrowth dynamics.^{7,21} Periods of axon extension, retraction and stalling can all be explained based on the balance of these forces. When axons are extending, $F_p > F_s + F_m$, and alternatively, when axons are retracting, the contractile forces are greater than the force of polymerization, thus $F_p < F_s + F_m$. Lastly, if axon outgrowth is stalled, there is a balance of forces such that $F_p = F_s + F_m$. During MII inhibition, we notice that for all substrates, axons which were initially extending continue to extend with similar outgrowth rates, meaning $F_p > F_s$. On the other hand, when axons are stalled and MII is inhibited, we see rapid extension because the polymerization force greatly exceeds that of the integrin and substrate-mediated traction forces, such that $F_p \gg F_s$. Microtubule engorgement has been observed on laminin substrates; however the rate of axon extension was not increased,³⁰ which the authors attribute to decreased substratum attachment. In our system, it is possible that the rapid engorgement of microtubules into the growth cone triggers enough force in the leading growth cone to encourage rapid extension. For cells which were already extending, this engorgement force may not be as dramatic, since the polymerization force

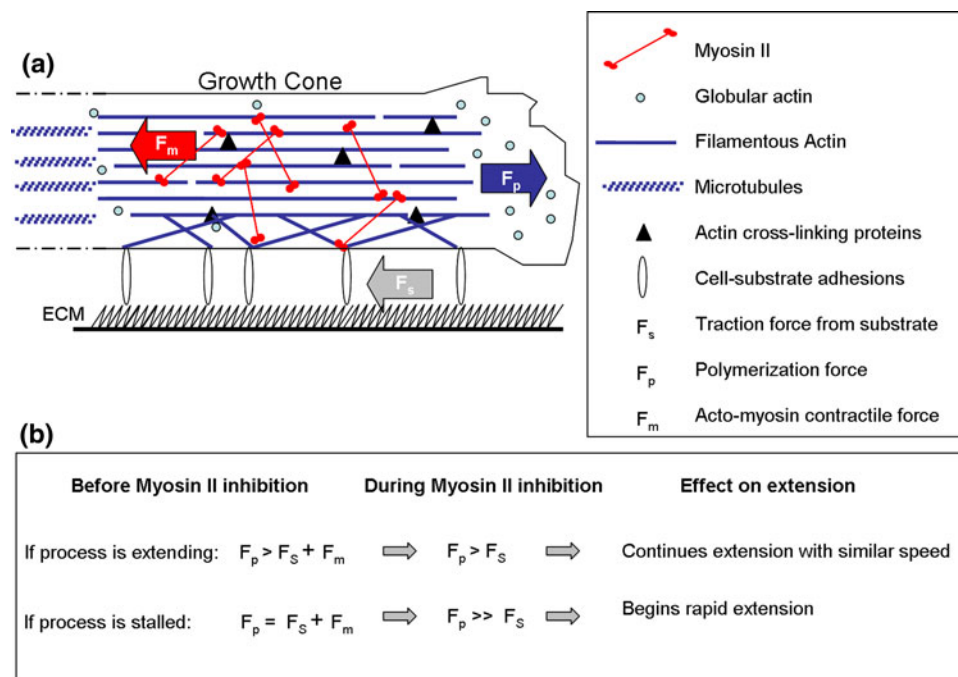


FIGURE 10. A simplified schematic illustrating some of the major cytoskeletal components and forces involved in axon extension and retraction (a). Three major forces in the growth cone arise from the traction force the cell exerts on the substrate (F_s) and extracellular matrix (ECM), the force of polymerizing actin filaments at the leading edge (F_p), and acto-myosin contractile forces which are involved in both axon extension and retraction (F_m). The effects of MII inhibition on axon outgrowth can be explained based on the balance of forces within the cell (b). When cells are initially extending prior to the addition of MII, the polymerization forces are greater than opposing traction and contractile forces, therefore the cell favors extension. When the process is stalled, however, the forces remain balanced, meaning the polymerization force is equal to the traction and contractile forces. During MII inhibition, the acto-myosin contractile force is compromised and extension is favored. This is consistent with our observations that during MII inhibition cells which were initially extending continue to extend, while cells which were previously stalled also begin to extend rapidly.

at the leading edge of the growth cone was already contributing to axon extension, therefore the growth rate continues unaffected. These results emphasize the critical balance in forces necessary for proper outgrowth dynamics and also suggest the ability to encourage axon extension from a previously stationary state. This results have important implications for various therapeutic techniques and tissue engineering applications, such as the encouragement of axon outgrowth across engineering platforms in the spinal cord.⁴³

CONCLUSION

This paper demonstrates that cortical neurons differentiate and extend processes similar in length and number on substrates of varying stiffness. Also, cortical extension and retraction dynamics, as well as myosin activity, are all independent of substrate stiffness. We observe only morphological differences between laminin vs. PDL-coated substrates; however, we do not observe any substrate dependent effects.

These results demonstrate that, unlike DRG (Fig. 5; Balgude *et al.*² and Willits and Skornia⁶²) and hippocampal³¹ neurons, cortical neuron behavior is not affected by substrate compliance. We hypothesize that this mechano-insensitivity results from the homogeneous environment of the developing cortex. Ultimately, the results presented here emphasize that mechanotactic behavior is cell type specific, and the native environment of the cell likely dictates its response to modifications in mechanical properties.

ACKNOWLEDGMENTS

This work was supported by NSF Grant CMMI-0643783 to HAE. We thank the Functional Macromolecular Laboratory at the University of Maryland (specifically Dr. Peter Kofinas and Brendan Casey) for training and use of the Dynamic Mechanical Analyzer. We would like to thank Kimberly Stroka for use of the custom-written Matlab programs used to fit AFM force curves, and Emily Shih and Hema Balkaran for

assistance with the cell body displacement and outgrowth analysis. We also thank Dr. Herbert Geller for stimulating discussions.

REFERENCES

- ¹Bagnard, D., *et al.* Axonal surface molecules act in combination with semaphorin 3a during the establishment of corticothalamic projections. *Cereb. Cortex* 11(3):278–285, 2001.
- ²Balgude, A. P., *et al.* Agarose gel stiffness determines rate of DRG neurite extension in 3D cultures. *Biomaterials* 22(10):1077–1084, 2001.
- ³Basarsky, T. A., V. Parpura, and P. G. Haydon. Hippocampal synaptogenesis in cell culture: developmental time course of synapse formation, calcium influx, and synaptic protein distribution. *J. Neurosci.* 14(11 Pt 1):6402–6411, 1994.
- ⁴Bentley, D., and A. Torioian-Raymond. Disoriented path-finding by pioneer neurone growth cones deprived of filopodia by cytochalasin treatment. *Nature* 323(6090):712–715, 1986.
- ⁵Billuart, P., *et al.* Regulating axon branch stability: the role of p190 RhoGAP in repressing a retraction signaling pathway. *Cell* 107(2):195–207, 2001.
- ⁶Boal, D. *Mechanics of the Cell.* Cambridge, UK: Cambridge University Press, p. 406, 2002.
- ⁷Bridgman, P. C., *et al.* Myosin IIB is required for growth cone motility. *J. Neurosci.* 21(16):6159–6169, 2001.
- ⁸Brown, X. Q., K. Ookawa, and J. Y. Wong. Evaluation of polydimethylsiloxane scaffolds with physiologically-relevant elastic moduli: interplay of substrate mechanics and surface chemistry effects on vascular smooth muscle cell response. *Biomaterials* 26(16):3123–3129, 2005.
- ⁹Chan, C. E., and D. J. Odde. Traction dynamics of filopodia on compliant substrates. *Science* 322(5908):1687–1691, 2008.
- ¹⁰Cheng, S., E. C. Clarke, and L. E. Bilston. Rheological properties of the tissues of the central nervous system: a review. *Med. Eng. Phys.* 30(10):1318–1337, 2008.
- ¹¹Clarke, E. C., S. Cheng, and L. E. Bilston. The mechanical properties of neonatal rat spinal cord in vitro, and comparisons with adult. *J. Biomech.* 42(10):1397–1402, 2009.
- ¹²Craig, A. M., and G. Banker. Neuronal polarity. *Annu. Rev. Neurosci.* 17:267–310, 1994.
- ¹³Dennerll, T. J., *et al.* The cytomechanics of axonal elongation and retraction. *J. Cell Biol.* 109(6 Pt 1):3073–3083, 1989.
- ¹⁴Dotti, C. G., C. A. Sullivan, and G. A. Banker. The establishment of polarity by hippocampal neurons in culture. *J. Neurosci.* 8(4):1454–1468, 1988.
- ¹⁵Elkin, B. S., *et al.* Mechanical heterogeneity of the rat hippocampus measured by atomic force microscope indentation. *J. Neurotrauma* 24(5):812–822, 2007.
- ¹⁶Engler, A. J., *et al.* Matrix elasticity directs stem cell lineage specification. *Cell* 126(4):677–689, 2006.
- ¹⁷Fiford, R. J., and L. E. Bilston. The mechanical properties of rat spinal cord in vitro. *J. Biomech.* 38(7):1509–1515, 2005.
- ¹⁸Flanagan, L. A., *et al.* Neurite branching on deformable substrates. *Neuroreport* 13(18):2411–2415, 2002.
- ¹⁹Franze, K., *et al.* Neurite branch retraction is caused by a threshold-dependent mechanical impact. *Biophys. J.* 97(7):1883–1890, 2009.
- ²⁰Gallo, G. Myosin II activity is required for severing-induced axon retraction in vitro. *Exp. Neurol.* 189(1):112–121, 2004.
- ²¹Gallo, G., H. F. Yee, Jr., and P. C. Letourneau. Actin turnover is required to prevent axon retraction driven by endogenous actomyosin contractility. *J. Cell Biol.* 158(7):1219–1228, 2002.
- ²²Georges, P. C., *et al.* Matrices with compliance comparable to that of brain tissue select neuronal over glial growth in mixed cortical cultures. *Biophys. J.* 90(8):3012–3018, 2006.
- ²³Georges, P. C., *et al.* Increased stiffness of the rat liver precedes matrix deposition: implications for fibrosis. *Am. J. Physiol. Gastrointest. Liver Physiol.* 293(6):G1147–G1154, 2007.
- ²⁴Gonthier, B., C. Nasarre, T. Rudiger, and D. Bagnard. Protocol for the primary culture of cortical neurons. In: *New Methods for Culturing Cells from Nervous Tissues*, Vol. 1, edited by P. Poindron, P. Pigué, and E. Forster. Basel: Karger, 2005, pp. 12–22.
- ²⁵Greene, L. A. Nerve growth factor prevents the death and stimulates the neuronal differentiation of clonal PC12 pheochromocytoma cells in serum-free medium. *J. Cell Biol.* 78(3):747–755, 1978.
- ²⁶Ichihara, K., *et al.* Gray matter of the bovine cervical spinal cord is mechanically more rigid and fragile than the white matter. *J. Neurotrauma* 18(3):361–367, 2001.
- ²⁷Jay, P. Y., *et al.* A mechanical function of myosin II in cell motility. *J. Cell Sci.* 108(Pt 1):387–393, 1995.
- ²⁸Jiang, G., *et al.* Rigidity sensing at the leading edge through alphavbeta3 integrins and RPTPalpha. *Biophys. J.* 90(5):1804–1809, 2006.
- ²⁹Kawaguchi, Y., F. Karube, and Y. Kubota. Dendritic branch typing and spine expression patterns in cortical nonpyramidal cells. *Cereb. Cortex* 16(5):696–711, 2006.
- ³⁰Ketschek, A. R., S. L. Jones, and G. Gallo. Axon extension in the fast and slow lanes: substratum-dependent engagement of myosin II functions. *Dev. Neurobiol.* 67(10):1305–1320, 2007.
- ³¹Kostic, A., J. Sap, and M. P. Sheetz. RPTPalpha is required for rigidity-dependent inhibition of extension and differentiation of hippocampal neurons. *J. Cell Sci.* 120(Pt 21):3895–3904, 2007.
- ³²Lamoureux, P., R. E. Buxbaum, and S. R. Heidemann. Direct evidence that growth cones pull. *Nature* 340(6229):159–162, 1989.
- ³³Leach, J. B., *et al.* Neurite outgrowth and branching of PC12 cells on very soft substrates sharply decreases below a threshold of substrate rigidity. *J. Neural Eng.* 4(2):26–34, 2007.
- ³⁴Lemmon, V., *et al.* Neurite growth on different substrates: permissive versus instructive influences and the role of adhesive strength. *J. Neurosci.* 12(3):818–826, 1992.
- ³⁵Levental, I., P. C. Georges, and P. A. Janmey. Soft biological materials and their impact on cell function. *Soft Matter* 3:299–306, 2007.
- ³⁶Lin, L., *et al.* Cell compressibility studies utilizing non-contact hydrostatic pressure measurements on single living cells in a microchamber. *Appl. Phys. Lett.* 92:233901–233903, 2008.
- ³⁷Lo, C.-M., *et al.* Cell movement is guided by the rigidity of the substrate. *Biophys. J.* 79:144–152, 2000.

- ³⁸Lu, Y. B., *et al.* Viscoelastic properties of individual glial cells and neurons in the CNS. *Proc. Natl Acad. Sci. USA* 103(47):17759–17764, 2006.
- ³⁹Majno, G., and I. Joris. *Cells, Tissues, Disease: Principles of General Pathology*. Worcester: Blackwell Science, 1996.
- ⁴⁰Matsumoto, T., *et al.* Local elastic modulus of atherosclerotic lesions of rabbit thoracic aortas measured by pipette aspiration method. *Physiol. Meas.* 23(4):635–648, 2002.
- ⁴¹Mazuchowski, E., and L. Thibault. Biomechanical properties of the human spinal cord and pia matter. In: *2003 Summer Bioengineering Conference*. Key Biscayne, FL: American Society of Mechanical Engineers, 2003.
- ⁴²Miller, K., *et al.* Mechanical properties of brain tissue in-vivo: experiment and computer simulation. *J. Biomech.* 33(11):1369–1376, 2000.
- ⁴³Norman, L. L., K. M. Stroka, and H. Aranda-Espinoza. Guiding axons in the central nervous system: a tissue-engineering approach. *Tissue Eng. B Rev.* 15(3):291–305, 2009.
- ⁴⁴Norman, L., *et al.* Modification of cellular cholesterol content affects traction force, adhesion and cell spreading. *Cel. Mol. Bioeng.* 3(2):151–162, 2010.
- ⁴⁵Odde, D. J., *et al.* Stochastic dynamics of the nerve growth cone and its microtubules during neurite outgrowth. *Bio-technol. Bioeng.* 50(4):452–461, 1996.
- ⁴⁶Paszek, M. J., *et al.* Tensional homeostasis and the malignant phenotype. *Cancer Cell* 8(3):241–254, 2005.
- ⁴⁷Pelham, Jr., R. J., and Y. Wang. Cell locomotion and focal adhesions are regulated by substrate flexibility. *Proc. Natl Acad. Sci. USA* 94(25):13661–13665, 1997.
- ⁴⁸Peyton, S. R., and A. J. Putnam. Extracellular matrix rigidity governs smooth muscle cell motility in a biphasic fashion. *J. Cell. Physiol.* 204(1):198–209, 2005.
- ⁴⁹Prange, M. T., and S. S. Margulies. Regional, directional, and age-dependent properties of the brain undergoing large deformation. *J. Biomech. Eng.* 124(2):244–252, 2002.
- ⁵⁰Rakic, P. Specification of cerebral cortical areas. *Science* 241(4862):170–176, 1988.
- ⁵¹Rice, D. S., and T. Curran. Role of the reelin signaling pathway in central nervous system development. *Annu. Rev. Neurosci.* 24:1005–1039, 2001.
- ⁵²Rico, F., *et al.* Probing mechanical properties of living cells by atomic force microscopy with blunted pyramidal cantilever tips. *Phys. Rev. E Stat. Nonlin. Soft Matter Phys.* 72(2 Pt 1):021914, 2005.
- ⁵³Saha, K., *et al.* Substrate modulus directs neural stem cell behavior. *Biophys. J.* 95(9):4426–4438, 2008.
- ⁵⁴Shi, P., *et al.* Dynamic force generation by neural stem cells. *Cell. Mol. Bioeng.* 2(4):464–474, 2009.
- ⁵⁵Siechen, S., *et al.* Mechanical tension contributes to clustering of neurotransmitter vesicles at presynaptic terminals. *Proc. Natl Acad. Sci. USA* 106(31):12611–12616, 2009.
- ⁵⁶Stroka, K. M., and H. Aranda-Espinoza. Neutrophils display biphasic relationship between migration and substrate stiffness. *Cell Motil. Cytoskeleton* 66(6):328–341, 2009.
- ⁵⁷Tessier-Lavigne, M., and C. S. Goodman. The molecular biology of axon guidance. *Science* 274(5290):1123–1133, 1996.
- ⁵⁸Tischler, A. S., *et al.* Nerve growth factor is a potent inducer of proliferation and neuronal differentiation for adult rat chromaffin cells in vitro. *J. Neurosci.* 13(4):1533–1542, 1993.
- ⁵⁹Tucker, K. L., M. Meyer, and Y. A. Barde. Neurotrophins are required for nerve growth during development. *Nat. Neurosci.* 4(1):29–37, 2001.
- ⁶⁰Wang, Y. L., and R. J. Pelham, Jr. Preparation of a flexible, porous polyacrylamide substrate for mechanical studies of cultured cells. *Methods Enzymol.* 298:489–496, 1998.
- ⁶¹Weisenhorn, A. L., *et al.* Deformation and height anomaly of soft surfaces studied with an AFM. *Nanotechnology* 4:106–113, 1993.
- ⁶²Willits, R. K., and S. L. Skornia. Effect of collagen gel stiffness on neurite extension. *J. Biomater. Sci. Polym. Ed.* 15(12):1521–1531, 2004.
- ⁶³Wong, J. Y., *et al.* Directed movement of vascular smooth muscle cells on gradient-compliant hydrogels. *Langmuir* 19:1908–1913, 2003.
- ⁶⁴Wylie, S. R., and P. D. Chantler. Separate but linked functions of conventional myosins modulate adhesion and neurite outgrowth. *Nat. Cell Biol.* 3(1):88–92, 2001.
- ⁶⁵Yeung, T., *et al.* Effects of substrate stiffness on cell morphology, cytoskeletal structure, and adhesion. *Cell Motil. Cytoskeleton* 60(1):24–34, 2005.